^{2}H MAS NMR Studies of the Manganese Dioxide Tunnel Structures and Hydroxides Used as Cathode Materials in Primary Batteries

Younkee Paik, John P. Osegovic, Francis Wang,† William Bowden,‡ and Clare P. Grey*

Contribution form the Department of Chemistry, State University of New York at Stony Brook, Stony Brook, New York 11794-3400, Duracell Global Science Center, Danbury, Connecticut 06801, and Gillette Advanced Technology Center, U.S.A., Needham, Massachusetts 02494

Received April 11, 2001. Revised Manuscript Received July 3, 2001

Abstract: Variable-temperature ^{2}H MAS NMR spectroscopy was used to investigate the local environments and mobility of deuterons in the manganese dioxide tunnel structures. Five systems were investigated: electrolytic manganese dioxide (EMD), the model compounds groutite and manganite, and deuterium intercalated ramsdellite and pyrolusite. Ruetschi deuterons, located in the cation vacancy sites in EMD, were detected by NMR and give rise to a resonance at 150 ppm at room temperature. These deuterons are rigid on the ^{2}H MAS NMR time scale (i.e., the correlation time for motion, τ_c, is $>10^{-3}$ s) at room temperature, but start to become mobile above 150 °C. No Coleman protons (in the so-called 1 × 1 and 1 × 2 tunnels in EMD) were observed. Much larger ^{2}H NMR hyperfine shifts of ∼300 and ∼415 ppm were observed for the deuterons in the tunnel structures of manganite and groutite, which could be explained by considering the different bonding arrangements for deuterons in the 1 × 1 and 1 × 2 tunnels. The smaller shift of the EMD deuterons was primarily ascribed to the smaller number of manganese ions in the deuterium local coordination sphere. Experiments performed as a function of intercalation level for ramsdellite suggest that the 1 × 1 tunnels are more readily intercalated in highly defective structures. The almost identical shifts seen as a function of intercalation level for deuterons in both 1 × 1 and 1 × 2 tunnels are consistent with the localization of the e_g electrons near the intercalated deuterium atoms. A Curie−Weiss-like temperature dependence for the hyperfine shifts of EMD and groutite was observed with temperature, but very little change in the shift of the manganite deuterons was observed, consistent with the strong antiferromagnetic correlations that exist above the Néel temperature for this compound. These different temperature dependences could be used to identify manganite-like domains within the sample of groutite, which could not be detected by X-ray diffraction.

Introduction

Electrolytic manganese dioxide (EMD), a form of γ-MnO_2, is used worldwide as the cathode material in both lithium and alkaline primary (i.e., nonrechargeable) batteries. EMD is a highly disordered material, which consists of an intergrowth of the manganese oxides, ramsdellite (R-MnO_2, space group *Pbnm*)[1] and pyrolusite (β-MnO_2, space group $P4_2/mnm$)[2] (Figure 1a). The one-dimensional arrays of edge-sharing manganese octahedra in both ramsdellite and pyrolusite (and thus EMD) are arranged to form tunnel structures, which can incorporate cations such as protons and Li^+. The ramsdellite structure contains larger 1 × 2 tunnels, where the notation "1 × 2" indicates a rectangular shaped tunnel formed on one side by the faces of the double chains of edge-sharing MnO_6 octahedra and on the other by single octahedra. Smaller 1 × 1 tunnels are present in the pyrolusite structure.

The disorder in γ-MnO_2, which broadens and leads to selective extinction of certain X-ray diffraction reflections, is thought to be due to a variety of structural features beyond the simple ramsdellite−pyrolusite intergrowth model, including the presence of Mn(III) sites, cation vacancies, and twinning defects. At present there are four different structural models for EMD.[3−7] Chabre and Pannetier suggested a systematic way to characterize and classify γ-MnO_2 by introducing two parameters that quantify the number and types of structural defects in the intergrowth structure: namely the parameter "p_r", which represents the fraction of pyrolusite domains in a ramsdellite-based structure (the De Wolf disorder), and "T_w" (the microtwinning), which represents the number of faults generated by twinning planes in both pyrolusite and ramsdellite domains.[7]

EMD generally contains ∼4 wt % of structural water in the crystal structure, which dramatically influences not only electrochemical properties but also other properties such as the density and electronic conductivity.[8] Many studies have been performed to explore the relationship between structural water content and various physical, chemical, and electrochemical properties of the electrochemically active MnO_2 forms.[9] The cation vacancy model, originally proposed by Ruetschi, is the most successful model for explaining many of these properties. In this model, the presence of protons associated with cation

* Address correspondence to this author at the State University of New York at Stony Brook.
† Duracell Global Science Center.
‡ Gillette Advanced Technology Center.

(1) Bystrom, A. M. *Acta Chem. Scand.* **1949**, *3*, 163.
(2) Baur, W. H. *Acta Crystallogr.* **1976**, *32*, 2200.
(3) De Wolff, P. M. D. *Acta Crystallogr.* **1959**, *12*, 341.
(4) Heuer, A. H.; He, A.; Hughes, P.; Feddrix, F *ITE Lett.* **2000**, *1* (6), B50.
(5) Simon, D. E.; Anderson, T. N.; Elliott, C. D. F *ITE Lett.* **2000**, *1* (3), B1.
(6) Bowden, W.; Sirotina, R.; Hackney, S. *IBA Lett.* **2000**, *1* (6), B27.
(7) Chabre, Y.; Pannetier, J. *Prog. Solid State Chem.* **1995**, *23*, 1.
(8) Tvarusko, A. *J. Electrochem. Soc.* **1964**, *111*, 125.
(9) Anderson, T. In *Modern Aspects of Electrochemistry*; White, R. E., et al., Eds.; Plenum Press: New York, 1996; No. 30, pp 313-413.

10.1021/ja015999k CCC: $20.00
Published on Web 08/30/2001

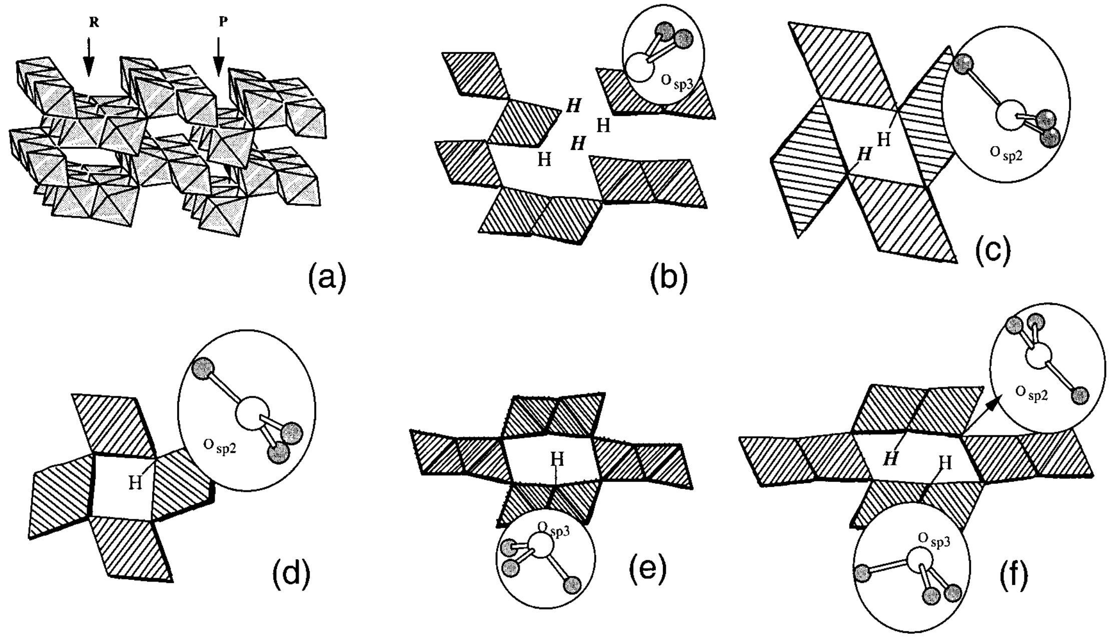

Figure 1. Schematic representation of (a) the structure of EMD, where "R" represents ramsdellite and "P" pyrolusite domains, and (b) suggested sites for "Ruetschi" protons in the manganese vacancies.[10] (c) The structure of manganite[16] and proton sites as determined by a neutron diffraction study.[17] (d) The structure of pyrolusite[2] and possible sites for intercalated protons. (e) The structure of ramsdellite[1] and suggested sites for protons at a reduction level of <0.5, i.e., $MnOOH_x$ ($0 < x < 0.5$).[21] (f) The X-ray structure of groutite and suggested sites for protons.[19] The atomic positions for the two proton sites, in the *c*-direction, in (b), (c), and (f) are $z = 0$ for "H" and $z = {}^1/_2$ for "***H***". The approximate geometries of the oxygen atom bonded to the protons are shown in circles, the atoms with a smaller radius representing manganese.

vacancies, the "Ruetschi" protons (Figure 1b), are proposed to provide a quantitative explanation of the cathode's capacity.[10−12] These protons are associated with nearby Mn^{4+} cations. Other protons, termed "Coleman" protons, which are associated with Mn^{3+} cations in the tunnels of the EMD structure, have also been suggested; these were proposed (by Ruetschi) to be more mobile than Ruetschi protons. Chabre and Pannetier, however, have pointed out that there is no evidence for the two distinct sets of protons. These protons can, however, be clearly distinguished from those in the form of molecular water adsorbed on the microporous surface of EMD, since the latter are removed at ~150 °C, while the former are removed progressively by heating at temperatures between ~150 and 400 °C.[12] Chabre and Pannetier, in their microtwinning model, have also proposed different crystallographic environments for the cation vacancies from those proposed in Ruetschi's model, the vacancies concentrating in the Mn sites in the twin plane; the shorter $Mn^{4+}-Mn^{4+}$ distances than those found in the regular lattice were proposed to destabilize the MnO_6 octahedra, lowering the energy for vacancy formation.[7]

The magnetic properties of manganese dioxide and hydroxide phases have been extensively studied, and the magnetic susceptibility (χ) has been shown to increase from pyrolusite to γ-MnO_2.[13] Variable-temperature magnetic studies on these systems show that strong antiferromagnetic (AF) couplings between manganese ions persist at ambient temperatures (i.e., well above the Néel temperature) and are responsible for a reduction in the magnetic moments of the manganese ions from those predicted from the spin-only formula. This coupling is extremely strong in pyrolusite (β-MnO_2; Néel temperature 84 K[14]) and manganite (γ-MnOOH; Néel temperature 45 K[15]).

Despite much work in this field, many unanswered questions remain as to the exact location and nature of these protons, which have direct bearing on why some EMD preparations produce materials that function as high-capacity primary batteries, while others show very poor electrochemical behavior.[9] The poor crystallinity of EMD and ramsdellite has prevented accurate structural determination of the positions of the protons in these materials by diffraction methods.[7] In this present work, we apply ^2H solid-state magic angle spinning (MAS) NMR spectroscopy to investigate the electronic and magnetic environments of the protons in EMD and related materials. We show that we can detect the ^2H resonance of the Ruetschi protons, allowing both the mobility of these deuterons and their local environment to be probed. For comparison, deuterated forms of two different manganese hydroxides with relatively well-determined crystal structures, manganite (γ-MnOOH, space group $B2_1/d$)[16,17] and groutite (α-MnOOH, space group *Pbnm*),[18−20] were also investigated. ^2H MAS NMR spectra were acquired from partially reduced samples of the manganese dioxide tunnel structures, pyrolusite and ramsdellite, to probe the changes in structural and electronic local environments of the deuterons during the reduction pathways of these systems. Figure 1c−f shows the schematic structures of the model compounds investigated and their suggested proton sites from X-ray and/or neutron diffraction studies.[1,2,17,19,21]

^2H NMR spectroscopy has been widely used to study a variety of solid systems including polymers,[22] biological molecules,[23]

(10) Ruetschi, P. *J. Electrochem. Soc.* **1984**, *131*, 2737.
(11) Ruetschi, P. *J. Electrochem. Soc.* **1988**, *135*, 2657.
(12) Ruetschi, P.; Giovanoli, R. *J. Electrochem. Soc.* **1988**, *135*, 2663.
(13) Moore, T. E.; Ellis, M.; Selwood, P. W. *J. Am. Chem. Soc.* **1950**, *72*, 856.
(14) Bizette, H.; Tsai, B. *Proceedings of the Conference on the Polarization of Matter*; Paris, April 4−9, 1949.
(15) Dachs, H. *Int. J. Magn.* **1973**, *4* (1), 5.
(16) Buerger, M. J. *Z. Kristallogr.* **1936**, *95*, 163.
(17) Dachs, H. *Z. Kristallogr.* **1963**, *118*, 303.
(18) Gruner, J. W. *Am. Min.* **1947**, *32*, 654.
(19) Glasser, L. S. D.; Ingram, L. *Acta Crystallogr.* **1968**, *B24*, 1233.
(20) Collin, R. L.; Lipscomb, W. N. *Acta Crystallogr.* **1949**, *2*, 104.
(21) Maskell, W. C.; Shaw, J. E. A.; Tye, F. L. *Electrochim. Acta* **1981**, *26*, 1403.
(22) Spiess, H. W. *Colloid Polym. Sci.* **1983**, *261*, 193.

and inorganic materials[24,25] to probe both structure and dynamics. ^{2}H is a spin 1 quadrupolar nucleus and the ^{2}H NMR spectra of diamagnetic materials are typically dominated by the quadrupolar interaction. The quadrupolar interaction broadens the spectra resulting in characteristic (Pake-doublet) symmetric line shapes.[26] Motion in the time scale of this interaction, which is determined by the size of the ^{2}H quadrupole coupling constant (QCC, typically 160−240 kHz for an O−D environment in an inorganic solid),[24,25,27,28] results in a narrowing of the broad line shape; different types of motion (e.g., rotation about a particular molecular axis, librations, etc.) can often be distinguish by careful analysis of the ^{2}H NMR line shape. Rapid motion in the so-called fast-regime, involving complete averaging about three perpendicular axes, results in a single sharp isotropic resonance. Experiments are typically performed by using a quadrupolar-echo sequence, and thus motion on a time scale determined by the evolution period of this sequence (typically 20−200 μs) results in a dramatic loss of signal intensity. Both the sensitivity and the resolution of ^{2}H NMR may be improved dramatically by using MAS (Magic Angle Spinning).[29] This is particularly important in the EMD systems, which contain low concentrations of deuterons. MAS, however, complicates the analysis of motion. Now, any motion in the time scale of the rotation frequency will prevent refocusing at the rotor echo and may result in dramatic line broadening and an apparent loss of signal intensity.[30]

The systems under investigation are all paramagnetic, which further complicates the analysis of the spectra: spectra of paramagnetic materials are typically strongly influenced by the large interaction between the unpaired electrons and the nuclear spins, which can shift the resonances significantly from the typical chemical shift ranges expected for diamagnetic materials and result in large spinning sideband manifolds and/or line broadening. The dipolar interaction between nuclear and electronic spins is directly proportional to the gyromagnetic ratio of the nucleus, and thus is almost an order of magnitude smaller for ^{2}H than ^{1}H. Relaxation mechanisms are also less effective as a consequence of the smaller coupling, and ^{2}H MAS has been shown to yield significantly improved resolution as compared to ^{1}H MAS NMR spectra, for paramagnetic solids.[31] Our earlier attempts to obtain ^{1}H MAS NMR from the EMD systems did not yield spectra that could be readily interpreted, hence the use of ^{2}H MAS NMR in the work presented here.

The ^{2}H line shapes of paramagnetic materials have been analyzed by a number of authors, and the combination of the quadrupolar interaction and the interaction between the ^{2}H and the paramagnetic ions has been shown to result in asymmetric line shapes[25,32] or asymmetric spinning sideband manifolds in MAS NMR spectra. The ^{2}H NMR line shapes depend not only on the strength of both quadrupole and paramagnetic dipolar interactions but also on the mutual orientation of their principal axes systems (PASs).[28]

Experimental Section

Synthesis. (a) EMD and Groutite: A deuterated EMD sample was synthesized by electrolysis of a solution of 0.8 M $MnSO_4$ and 0.5 M H_2SO_4 in D_2O at ∼6.5 mA/cm^2 at 95 °C. The particle size ranges from 1 to 100 μm with the average being ∼40 μm. The average manganese oxidation state is +3.92(0.01), based on titration of samples prepared under identical conditions but with nondeuterated reagents.

Two different deuterated groutite (α-MnOOD) samples were synthesized by heating a 1:1.5 molar ratio of either the International Battery Association No. 20 (IBA20) EMD sample or ramsdellite and deuterium-exchanged cinnamyl alcohol in a round-bottomed flask at 80 °C in xylene for 2 days.[33] Cinnamyl alcohol, C_9H_9OD (mp = 33−35 °C), deuterated at the hydroxyl group was obtained by dissolving the alcohol in D_2O and stirring at room temperature for 24 h followed by a filtration and evaporation under vacuum at ∼0 °C. A high level of deuteration was achieved, as confirmed by the significant (>80%) reduction of the resonance from the hydroxyl proton in the ^{1}H NMR spectrum of the product. IBA20 was provided by Duracell, Inc. and is an IBA sample specimen. The artificial ramsdellite was a generous gift of Dr J. C. Rousche of ERACHEM. The deuterated groutite samples were well washed with diethyl ether and dried under vacuum at 40 °C for 24 h.

A similar procedure was used to partially reduce ramsdellite, but now different temperatures of 20 or 50 °C for 5 h, with the same MnO_2:cinnamyl alcohol molar ratio as above, were used. The products were well washed and dried under vacuum at 40 °C for 24 h, and a small portion of each product was kept in a sealed bottle under N_2(g) atmosphere for 6 months to investigate the effect of time on the proton (and deuteron) distributions.

(b) Pyrolusite and Manganite: Deuterated manganite (γ-MnOOD) was synthesized following the same method used by Lee et al.,[34] but here D_2O, instead of H_2O, was used for deuteration. Aqueous ammonia (75 mL, 0.2 M in D_2O) was added dropwise to a solution of manganous sulfate (2.5 g in 250 mL of D_2O) and hydrogen peroxide (5 mL, 30% w/v) at room temperature, which was then refluxed at 100 °C for 26 h and filtrated. The solid product was dried in air at 100 °C.

Deuterium intercalation into the 1 × 1 tunnel structure of pyrolusite (purchased from Fisher Scientific) was carried out by heating the sample with an excess of deuterium-exchanged cinnamyl alcohol in xylene at 80 °C for 4 days. The product was washed with ether and dried under vacuum at 40 °C for 24 h.

Characterization. (a) Magnetic Susceptibility Measurements: These measurements were carried out with the Johnson Matthey Evans balance to check the reduction level of some of the samples. Mercury-(II) tetrathiocyanatocobaltate(II), $HgCo(SCN)_4$, was used as a calibration standard.

(b) X-ray diffraction: Data were collected on a Scintag powder X-ray diffractometer (Cu Kα radiation); all the diffraction patterns were compared with those in the Joint Committee on Powder Diffraction Standards (JCPDS).

(c) NMR: ^{2}H MAS NMR experiments were performed at 30.73 MHz on a CMX-200 spectrometer with Chemagnetics probes equipped with 4 or 5 mm rotors for MAS. Spectra were recorded with a rotor synchronized Hahn-echo pulse sequence, with evolution periods of one rotor period. The deuterium 90° pulse length was 2.9 μs, the dwell time was 1 μs, and the recycle delay ranged from 100 to 400 ms, depending on the compound and the temperature. The MAS speed varied from 9 to 18 kHz. All spectra were referenced to D_2O at 4.8 ppm as an external reference.

Results

X-ray Diffraction and Magnetic Susceptibility Measurements. The X-ray diffraction (XRD) powder patterns of the deuterated groutite and the partially reduced ramsdellites are compared with those in JCPDS in Figure 2. The artificial ramsdellite samples are poorly crystalline, and contain consider-

(23) Griffin, R. G. In *Methods in Enzymology*; Lowenstein, J. M., Ed.; Academic Press: San Diego, 1981; Vol. 72, p 108.
(24) Wittebort, R. J.; Usha, M. G.; Ruben, D. J.; Wemmer, D. E.; Pines, A. *J. Am. Chem. Soc.* **1988**, *110*, 5668.
(25) Lin, T.; DiNatale, J. A.; Vold, R. R. *J. Am. Chem. Soc.* **1994**, *116*, 2133.
(26) Pake, G. E. *J. Chem. Phys.* **1948**, *16*, 327.
(27) Gupta, L. C.; Setty, D. L. R. *J. Phys. Soc. Jpn.* **1969**, *26*, 1065.
(28) Lee, H.; Polenova, T.; Beer, R. H.; McDermott, A. E. *J. Am. Chem. Soc.* **1999**, *121*, 6884.
(29) Ackerman, J. L.; Eckman, R.; Pines, A. *Chem. Phys.* **1979**, *42*, 423.
(30) Maricq, M. M.; Waugh, J. S. *J. Chem. Phys.* **1979**, *70*, 3300.
(31) Liu, K.; Ryan, D.; Nakanishi, K.; McDermott, A. *J. Am. Chem. Soc.* **1995**, *117*, 6897.
(32) Siminovitch, D. J.; Rance, M.; Jeffrey, K. R. *J. Magn. Reson.* **1984**, *58*, 62.
(33) Gabano, J. P.; Morignat, B.; Fialdes, E.; Emery, B.; Laurent, J. F. *Z. Phys. Chem.* **1965**, *46*, 359.
(34) Lee, J. A.; Newnham, C. E.; Stone, F. S.; Tye, F. L. *J. Solid State Chem.* **1980**, *31*, 81.

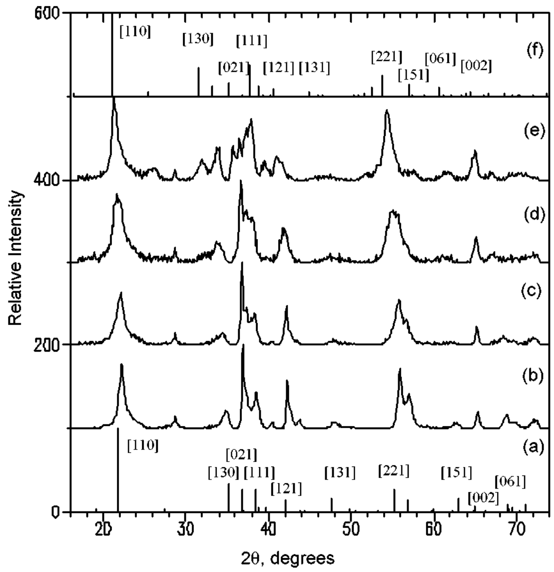

Figure 2. X-ray powder diffraction patterns of (a) natural ramsdellite, JCPDS file #390375, (b) artificial ramsdellite, (c) partially reduced ramsdellite ($MnOOD_{0.5}$), (d) partially reduced ramsdellite ($MnOOD_{0.7}$), (e) deuterated groutite, and (f) natural groutite, JCPDS file #751199.

able disorder; the crystallinity/disorder level of our samples is, nonetheless, similar to typical samples in the literature.[35] A weak reflection at 28.5° in 2θ is due to pyrolusite impurities.[7] Rietveld analysis of the ramsdellite XRD pattern suggests a composition of ca. 89% ramsdellite and 11% pyrolusite. The diffraction patterns show gradual shifts of all the peaks to lower 2θ values on intercalation, which is ascribed to the expansion of the unit cell and distortion of the 1×2 tunnel structures caused by reduction and deuteron intercalation into the tunnels, and indicates that reduction of ramsdellite has been achieved.[36]

Magnetic susceptibility measurements were carried out to check the reduction level of the partially reduced ramsdellite. Magnetic moments, μ_n, of the host compound (ramsdellite) and the fully reduced compound (groutite) were 2.61 and 2.99, respectively, in units of Bohr magneton (μ_B). The average oxidation state of the manganese ions changes from $Mn^{4+}(d^3)$ in ramsdellite to Mn^{3+}(high-spin d^4) in groutite, and thus, these experimental values are lower than those expected based on the number of unpaired electrons in each compound (typical experimental values for d^3 and d^4 (high-spin) ions are 3.87 and 4.90 μ_B, respectively). These lower values are ascribed to short-range antiferromagnetic (AF) couplings between manganese ions, which persist well above the Néel temperature.[37] By assuming that the (reduced) magnetic moment of the manganese atom in this range of oxidation states is still proportional to the number of unpaired electrons in each manganese ion, we can use an empirical formula to estimate the level of reduction (x) per MnO_2 formula unit due to proton insertion per MnO_2 unit:

$$\mu_n(d^{3+x}) = \mu_n(d^3) + x\{\mu_n(d^4) - \mu_n(d^3)\},\ 0 \le x \le 1$$

where $\mu_n(d^{3+x})$ is the magnetic moment of the partially reduced manganese hydroxide, with an average number of d-electrons per manganese ion of $3 + x$ (assuming high-spin manganese ions). Values of $x = 0.5$ and 0.7 are calculated for the samples prepared at 20 and 50 °C, based on the measured values for $\mu_n(d^{3+x})$ of 2.80 and 2.89 μ_B, leading to values for the average oxidation states of manganese of $Mn^{3.5+}$ and $Mn^{3.3+}$, respectively. For convenience, the approximate corresponding molecular formulas of the reduced compounds, $MnOOD_{0.5}$ and $MnOOD_{0.7}$, will be used henceforward.

The powder XRD pattern of deuterated manganite shows a series of sharp reflections corresponding to highly crystalline manganite. Weaker reflections at 33°, 36°, 38°, 58°, and 59° in 2θ were also observed, which could be indexed to γ-Mn_2O_3. This is consistent with an earlier study, where reflections corresponding to a γ-Mn_2O_3 impurity were also observed in the powder XRD data of a synthetic manganite sample.[34] No significant change was observed between the powder XRD pattern of deuterium-intercalated pyrolusite and that of the host compound (pyrolusite); sharp reflections were observed in both patterns, and no significant loss in crystallinity was observed on intercalation.

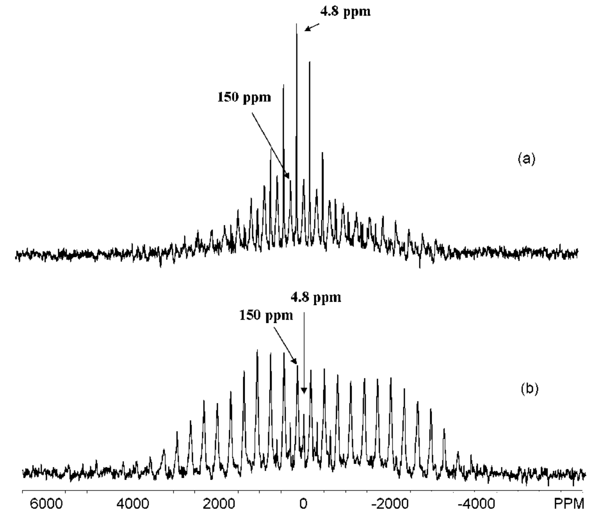

Figure 3. The ^{2}H MAS NMR spectra of deuterated EMD (a) dried at 60 °C for 24 h under vacuum and (b) dried at 90 °C for 24 h under vacuum after having acquired spectrum a. The isotropic peaks are marked with the corresponding NMR shifts. A spinning speed of 9.5 kHz and a spin−echo were used to acquire both spectra.

^{2}H MAS NMR. (a) Deuterated EMD: Two isotropic resonances with large sideband manifolds are observed in the ^{2}H MAS NMR spectra of the deuterated EMD (Figure 3). The isotropic resonance at 4.8 ppm shows the same NMR shift as that of liquid water and the intensity of this resonance decreased dramatically after further heat treatment at 90 °C (Figure 3b). Hence, we assign this resonance to molecular water adsorbed on the microporous surface of EMD, since desorption of this water mostly occurs below ∼150 °C.[12] The spectrum is dominated by a second resonance with a large isotropic shift (150 ppm) and a wide, asymmetric sideband envelope, due to deuterium spins in an asymmetric paramagnetic environment. We assign this resonance to the "Ruetschi" deuterons. The much smaller set of spinning sidebands for the resonance assigned to water molecules indicates that these molecules are mobile. The Ruetschi deuterons are rigid in the time scale of the ^{2}H MAS NMR experiment.

(b) Deuterated groutite, manganite, and pyrolusite: ^{2}H MAS NMR spectra were acquired from the two different groutites synthesized from different starting materials, IBA20 and ramsdellite (Figure 4). Four isotropic resonances are observed in each spectrum. The isotropic resonance at ∼0−5 ppm decreases in intensity on drying at moderate temperatures (∼90 °C) and is assigned to molecular water adsorbed on the surface or captured in the micropores of groutite.

(35) Thackeray, M. M.; Rossouw, M. H.; Gummow, R. J.; Liles, D. C.; Pearce, K.; De Kock, A.; David, W. I. F.; Hull, S. *Electrochim. Acta* **1993**, *38*, 1259.
(36) Fitzpatrick, J.; Tye, F. L. *J. Appl. Electrochem.* **1991**, *21*, 130.
(37) Grey, J. T. *J. Am. Chem. Soc.* **1946**, *68*, 605.

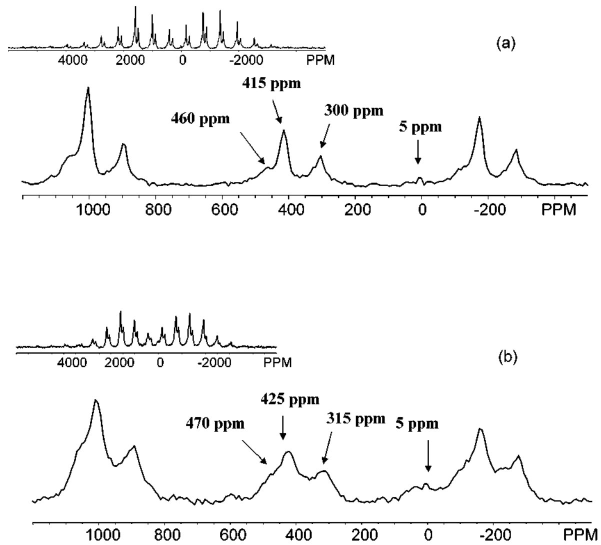

Figure 4. The full ^2H MAS NMR spectra, together with an expanded region, of the deuterated groutites: (a) synthesized from ramsdellite and (b) synthesized from IBA20. Spectra were acquired at a spinning speed of 18 kHz. Centerbands are marked with the corresponding isotropic chemical shifts.

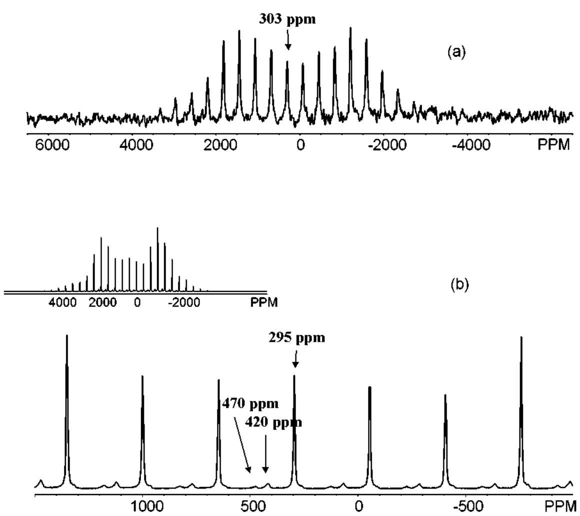

Figure 5. The ^2H MAS NMR spectra of (a) deuterium intercalated pyrolusite and (b) deuterated manganite. The isotropic resonances are marked with the corresponding NMR shifts. Both spectra were acquired at a spinning speed of ~11 kHz.

Two different types of oxygen atoms are present in the groutite (α-MnOOH) structure (Figure 1f).[19] The first one is surrounded by three manganese atoms in a roughly coplanar triangle; we denote this oxygen O_{sp^2}, because the geometry corresponds to sp^2 hybridization of the oxygen atom. The second oxygen atom forms the apex of a trigonal pyramid whose base consists of three manganese atoms and is denoted O_{sp^3}. Based on the $O_{sp^3}-O_{sp^2}$ distances determined in an earlier X-ray diffraction study, it was proposed that the proton is directly coordinated to O_{sp^3}, but also forms a hydrogen bond to O_{sp^2}.[7,19,21] The isotropic resonances arising at ~415 ppm (415 ppm in Figure 4a and 425 ppm in Figure 4b) have the highest intensities in the ^2H NMR spectra of groutites. Thus, we assign these resonances to the deuterons bonded to the pyramidal oxygen (O_{sp^3}) in the 1×2 tunnels of groutite.

The ^2H MAS NMR spectra of deuterated pyrolusite and manganite are shown in Figure 5. Manganite and pyrolusite have isomorphic 1×1 tunnel structures (Figure 1c,d). The similar ^2H NMR shifts (~300 ppm) of the isotropic resonances in each spectrum and the similar sideband patterns suggest similar local environments for the deuterons in each of these two 1×1 tunnel structures. Thus, we assign the isotropic resonance at ~300 ppm in each spectrum to deuterons in the 1×1 tunnels of manganite and pyrolusite. The shift mechanisms responsible for these large shifts are discussed in a later section.

Two more isotropic resonances are observed in Figure 5b at 420 and 470 ppm, respectively. Synthetic manganite is reported to contain a small amount of groutite,[34] and the isotropic resonance at 420 ppm in Figure 5b shows a similar ^2H NMR shift the isotropic NMR resonance assigned to the deuterons in the 1×2 tunnels of groutite. Hence, we assign this resonance to the deuterons in groutite impurities. An isotropic resonance at ~470 ppm was also observed in the ^2H NMR spectra of groutite (Figure 4). As mentioned above, the powder XRD pattern of the deuterated manganite contains a small amount of γ-Mn_2O_3 as an impurity. But, this compound contains no protons (or deuterons) in the structure. Thus, we tentatively assign the isotropic resonances, observed at ~470 ppm in both the deuterated groutite and manganite, to deuterons in local environments other than the 1×1 and 1×2 tunnels and the cation vacancies, which may include the 1×3 tunnels as observed earlier by high-resolution transmission electron microscopy[38] or other crystal defects.

(c) Impurities in groutite: The XRD patterns of groutite are broad, indicating considerable disorder, thus it is not surprising that a series of resonances is observed by NMR.[7] The resonances at ~300−315 and ~460−470 ppm are assigned to deuterons intercalated into the defect sites or into the impurities formed during the reduction of the host compounds. The resonance observed at ~300−315 ppm is close to that of intercalated pyrolusite and or manganite, and is assigned to deuterons in 1×1 tunnels. Manganite formation is observed by several XRD studies at a reduction level of $x \geq 0.6$ in electrochemical cells, the exact value of x varying among authors.[7] Thus the ~300−315 ppm resonance in the deuterated groutite samples is ascribed to manganite deuterons and/or the small manganite-like blocks formed by intercalation into the pyrolusite domains present in the starting materials.

(d) Partially reduced ramsdellites: Figure 6 shows the ^2H MAS NMR spectra of ramsdellites reduced to different reduction levels. The isotropic resonances at 2−5 ppm are assigned to micropore (molecular) water. Surprisingly, the resonance at 330 ppm is the most intense resonance at the lowest reduction level (Figure 6a). As the reduction level increased, the isotropic resonance at ~400−415 ppm begins to dominate. We have assigned the isotropic resonance at ~415 ppm to deuterons in the 1×2 tunnels of groutite and the one at ~300 ppm to deuterons in the 1×1 tunnels of manganite. This result appears to contradict previous work, where it has been shown that the 1×2 tunnels in γ-MnO_2 are reduced first, transforming to groutite, after which proton filling of the pyrolusite domains occurs resulting in manganite domains.[7] Another noticeable result is that the signal intensity in the ^2H NMR spectrum of $MnOOD_{0.5}$ is only about one thirtieth of the intensity from groutite, MnOOD. These observations will be discussed in more detail in a later section.

No noticeable differences between the ^2H MAS NMR spectra of the fresh sample and samples that had been aged for 6 months were observed. This time period was chosen based on previous literature, which suggested that these samples require considerable aging before a uniform distribution of protons is achieved

(38) Turner, S.; Buseck, P. R. *Nature* **1983**, *304*, 143.

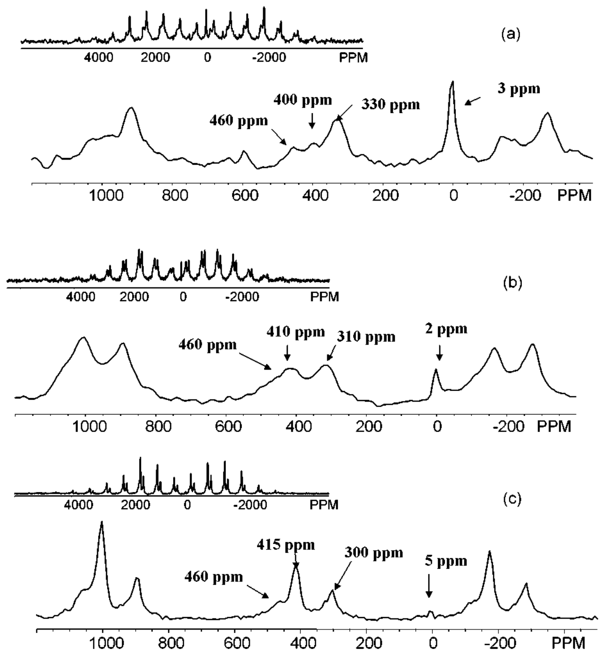

Figure 6. The full and expanded ^{2}H MAS NMR spectra of (a) partially reduced ramsdellite ($MnOOD_{0.5}$), where 1 499 792 transients were acquired, (b) partially reduced ramsdellite ($MnOOD_{0.7}$), where 303 168 transients were acquired, and (c) groutite ($MnOOD_{1.0}$) synthesized from ramsdellite, where 47 458 transients were acquired. Center bands are marked with corresponding isotropic chemical shifts. A spinning speed of ~18 kHz was used to acquire the spectra. All spectra are plotted on the same absolute intensity scale.

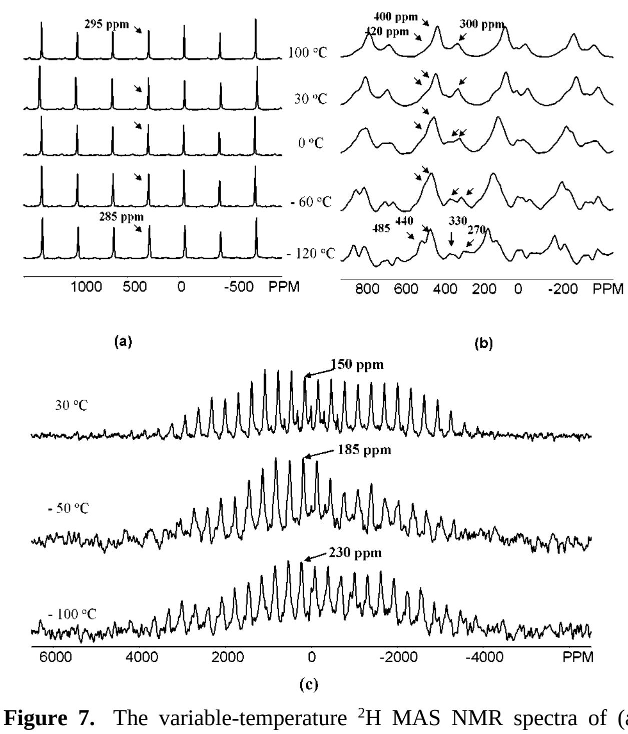

Figure 7. The variable-temperature ^{2}H MAS NMR spectra of (a) deuterated manganite, (b) deuterated groutite, and (c) deuterated EMD. The isotropic resonances are labeled. A MAS spinning speed of ~10 kHz was used.

throughout the lattice.[36] Our results indicate that this process, as probed by ^{2}H NMR, is not as slow as previously suggested.

(e) Variable-temperature NMR experiments: The variable-temperature (VT) ^{2}H NMR spectra are shown in Figure 7. The ^{2}H NMR shift of the isotropic resonance from EMD varies with temperature, and appears, based on the, albeit limited, temperature range investigated, to show a Curie−Weiss dependence on temperature, consistent with the magnetic susceptibility data for similar materials.[13] An approximate estimate for the Weiss constant of ~70 K can be extracted from a plot of 1/shift versus temperature (see Figure 8a), consistent with weak AF couplings between manganese ions.

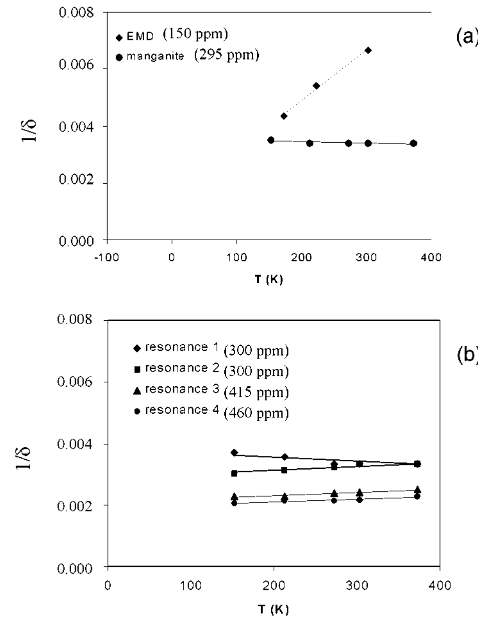

Figure 8. The inverse of the ^{2}H NMR shifts ($1/\delta$) as a function of temperature for (a) EMD and manganite and (b) groutite. The ^{2}H NMR shifts at 30 °C are marked for each resonance.

The ^{2}H NMR shift of the isotropic resonance in deuterated manganite shifts only very slightly to 285 ppm on cooling the sample from 100 down to ~120 °C. This behavior deviates considerably from the Curie−Weiss law, where the shift is expected to be proportional to $1/T$, but is consistent with the reported magnetic susceptibility (χ) data where no significant change in χ is observed in the temperature range investigated.[13]

The ^{2}H NMR spectrum of groutite acquired at −120 °C clearly shows that there are actually four or more different deuterium sites in this sample. Below 0 °C, the isotropic resonance at 300 ppm splits into two resonances (Figure 7b), one resonance shifting to higher frequency, the other resonance shifting slightly to lower frequency, as the temperature is decreased. On the basis of the VT ^{2}H NMR spectra of manganite (Figure 7a), we assign the isotropic resonance that shifts from 300 ppm at 100 °C to 270 ppm at −120 °C to deuterons in manganite impurities or large manganite-like domains. Figure 8b shows the temperature dependence of the ^{2}H NMR shifts of all the isotropic resonances of the deuterated groutite sample. The isotropic resonance assigned to deuterons in manganite domains (resonance 1) clearly shows a very different temperature dependence from all the other ^{2}H NMR isotropic resonances (resonances 2−4), but is similar to the temperature dependence of the isotropic resonance in manganite (Figure 8a), consistent with this assignment.

Groutite is synthesized from either artificial ramsdellite or EMD. Both materials contain intergrowths of 1 × 1 and 1 × 2 tunnel domains. When reduced, this intergrowth region is called δ-MnOOH.[7,36] On the basis of the shift, we, therefore, tentatively assign the isotropic resonance that shifts from 295 ppm at 100 °C to 330 ppm at −120 °C (resonance 2 in Figure 8b) to deuterons in the 1 × 1 tunnels of δ-MnOOH. These manganite (1 × 1) domains should be considerably smaller in size than those in manganite crystals, thus the magnetic interactions

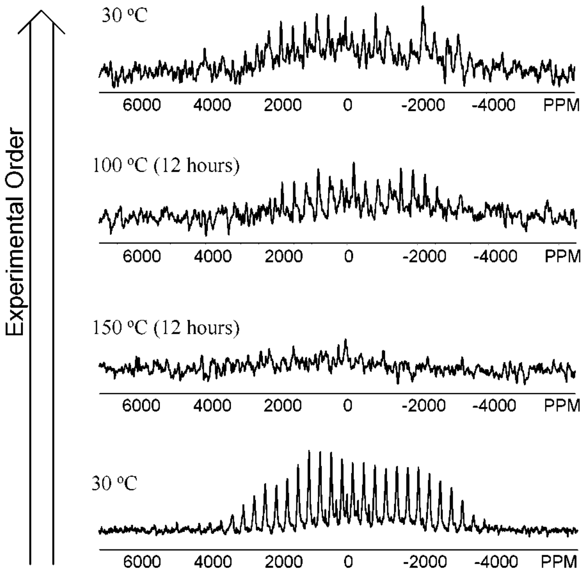

Figure 9. The variable-temperature ^{2}H MAS NMR spectra of EMD. The acquisition temperatures and times spent at each temperature are marked on each spectrum. A total of ~130 000 transients were acquired at a spinning speed of ~10 kHz. The order of the acquisition of the spectra is depicted by an arrow. All the spectra are plotted on the same intensity scale apart from the first spectrum, where the scale has been halved.

between manganese ions are not necessarily the same as those in bulk manganite. Indeed, the structural model for EMD of Bowden and Hackney[6] suggests that the pyrolusite domains in EMD consist of columns of 1 × 1 tunnels, instead of the slabs of 1 × 1 tunnels proposed in earlier models. The AF interactions between the manganese ions in the octahedra that form the 1 × 1 tunnels may be similar to those between manganese ions in the 1 × 2 domains. In short, the isotropic resonance at 300 ppm, which splits into two peaks, at 270 and 330 ppm at −120 °C, is due to two isotropic resonances, the first from deuterons in either large 1 × 1 domains or small manganite crystallites and the second from small manganite domains in intergrowth δ-MnOOD crystallites.

Figure 9 shows the ^{2}H MAS NMR spectra of EMD acquired between room temperature and 150 °C. A dramatic decrease in intensity was observed as the temperature was increased, and the signal at 150 °C was barely detectable. The sample was returned to 100 °C and then room temperature and an increase in signal intensity was observed and a few sidebands could be discerned in the ^{2}H MAS NMR spectra. The sample was then reheated and no signal could be detected at the highest temperature studied, 250 °C, even after acquiring 208 992 transients. Lattice water in EMD evaporates gradually above ~150 °C and the EMD converts to a pyrolusite-like form known as HEMD at around 350 °C.[9,12] Thus, the loss of signal intensity in the spectrum acquired at 150 °C is partially explained by the decrease in the amount of lattice deuterons on heating the sample. This does not explain the increase in the signal intensity on reducing the temperature from 150 °C to room temperature. When the motion of the Ruetschi deuterons, which can include reorientation and site exchange with nearby Ruetschi deuterons or (Coleman) deuteron sites, becomes comparable to the MAS NMR time scale, a loss of signal intensity is predicted.[30] A decrease in these motions can explain the gain in signal intensity on cooling the sample from 150 to 100 °C. In contrast, no dramatic changes were observed in the line shapes and intensities of the ^{2}H NMR spectra of manganite and groutite in the

Table 1. The Line Widths of the ^{2}H Resonances under MAS Conditions, as a Function of Temperature (in kHz)

temp (°C)	manganite	groutite	EMD	$MnOOD_{0.7}$
−100	0.29[a]	1.3[b]	2.0	2.6[b]
−60	0.29[a]	1.3[b]		
−50			1.6	
0	0.25[a]	1.3[b]		
30	0.25[a]	1.3[b]	1.3	1.9[b]
100	0.20[a]	1.1[b]	1.4	
150		0.91[b]	12[c]	

[a] Line width of the ~295 ppm resonance. [b] Line width of the ~415 ppm resonance. [c] Calculated from the FID echo train.

temperature range between −120 and 150 °C, suggesting that the deuterons in these materials are rigid on the NMR time scale.

(f) Line widths and spin−spin relaxation times: The line widths (full width at half-height) of the resonances of the individual peaks within the spinning sideband manifold were measured for groutite and manganite. In the case of EMD at 150 °C, the signal-to-noise was poor and thus the T_2* was measured by examining the intensities of the rotor echoes. The value was determined from the magnitude of the free induction decay, to help eliminate the effect of chemical shift offsets on the measured T_2*. The line width (given by $2/T_2$*) was then estimated. The results are summarized in Table 1. A number of trends are immediately apparent. First, the line widths of manganite are almost an order of magnitude smaller than those of EMD and groutite. Second, the line widths decrease slightly with temperature. A notable exception to this are the line widths of EMD which reach a minimum at room temperature but then increase dramatically as the temperature is raised further. T_2 values of 1.1 and 1.2 ms were measured for the resonances at 410 and 310 ppm, respectively, in $MnOOD_{0.7}$ by varying the evolution period of the spin−echo experiment. These T_2 values are shorter than the T_2* of manganite (8 ms) at room temperature, and essentially identical to the T_2* values of $MnOOD_{0.7}$ (1.1 and 1.2 ms for the 410 and 310 ppm resonances, respectively). The results indicate that only a very small contribution to the line widths of the resonances in this sample can come from a distribution in hyperfine shifts despite the noncrystalline nature of the material and the partial reduction level.

Discussion

Shift Mechanisms in Paramagnetic Systems. In related work, we[39] and Gee et al.[40] have shown that the lithium NMR shifts in manganese oxides result from a hyperfine, or Fermi-contact interaction. The magnitude and sign of this interaction depends on the atomic susceptibilities of the paramagnetic ions in the nearby coordination sphere of the NMR active nucleus, and the nature of the overlap between the manganese orbitals and s orbitals at the NMR active nucleus. The interaction may be either direct or mediated via an intervening oxygen atom (a transferred hyperfine shift). This latter mechanism is similar to the superexchange mechanism that can result in magnetic couplings between paramagnets.[41] The second shift mechanism, the pseudocontact shift, results from a coupling between the nuclear spin and an anisotropic magnetic moment.[42] A previous ^{1}H MAS NMR study of the paramagnetic cupric compound,

(39) Lee, Y. J.; Wang, F.; Grey, C. P. *J. Am. Chem. Soc.* **1998**, *120*, 12601.
(40) Gee, B.; Horne, C. R.; Cairns, E. J.; Reimer, J. A. *J. Phys. Chem. B* **1998**, *102*, 10142.
(41) Goodenough, J. B. *Magnetism and the Chemical Bond*; John Wiley & Sons: New York, 1963; pp 165−184.
(42) McConnell, H. M.; Robertson, R. E. *J. Chem. Phys.* **1958**, *29*, 1361.

$CuCl_2 \cdot 2H_2O$, reported a value for the ^1H pseudocontact shift of approximately 10 ppm,[43] which is small compared with the shifts observed in this system. Furthermore, unlike Cu^{2+}, the magnetic moments of Mn^{3+} ions, and Mn^{4+} ions in particular, are close to being isotropic.[44] For Mn^{3+}, recent high-frequency EPR studies of, for example, porphyrinic complexes have confirmed that $g_{\|} \approx g_{\perp} \approx 2.0$.[45] The pseudocontact shift mechanism will, therefore, be ignored in the subsequent discussion.

In our earlier lithium NMR work, we showed that the NMR hyperfine shifts could be readily rationalized by considering the different local environments surrounding the nuclear spins.[39,46] Thus, to rationalize the size of the Fermi contact shifts observed in this system, we need to consider the different local environment of the deuterons in these materials. In the manganite neutron diffraction structure, three Mn^{3+} ($t_{2g}^3e_g^1$) ions are directly coordinated to the protonated oxygen (O_{sp^2}) in the 1 × 1 tunnels, with Mn−O distances of 1.85 to 2.30 Å. Cation-(H^+)−anion($O_{sp^2}^{2-}$)−cation(Mn^{3+}) bond angles ranging from 90.4° to 110° (Figure 1c) were reported, the manganese ions around O_{sp^2} forming a roughly coplanar triangle (Figure 1c,d).[17] An O_{sp^2}−H bond distance of 1.022(0.020) Å was reported, indicating a covalent interaction of the proton with one oxygen atom. The ^2H NMR shift of ∼300 ppm of the deuterons in the 1 × 1 tunnels of either manganite or pyrolusite (Figure 5) can be attributed to a superexchange mechanism of the type shown in Figure 10a involving the half-filled manganese t_{2g} orbitals. Transfer of positive electron spin density from the half-filled t_{2g}-orbitals of the nearby three manganese ($t_{2g}^3e_g^1$) ions to the empty 1s-orbital of deuteron is mediated by a fully filled pσ oxygen (O_{sp^2}) orbital, resulting in a ^2H NMR hyperfine shift to higher frequency.[41,42] Since there is no overlap between the manganese e_g orbitals and the oxygen p-orbital coordinated to the deuteron for a 90° ^2H−O−Mn bond angle, the contribution to the shift due to any interactions involving the e_g orbitals will be small, and can be ignored to a first approximation. Given a ^2H NMR hyperfine shift of 295 ppm for the manganite deuteron at room temperature, each Mn^{3+} ion contributes approximately 295/3 ≈ 100 ppm to the hyperfine shift. In deuterium-intercalated pyrolusite, where only partial reduction of the manganese ions is expected, the local environment, at least at very low intercalation levels, is expected to contain only one Mn^{3+} ion and two Mn^{4+} ions directly bonded to deuterioxyl oxygen (O_{sp^2}). Nevertheless, the ^2H NMR shift of this deuteron is 303 ppm, quite similar to 295 ppm in manganite, which is consistent with the superexchange mechanism shown in Figure 10a, because this shift mechanism does not depend on the occupancy of the e_g-orbitals. Interestingly, recent IR (and inelastic neutron scattering, INS) studies have suggested that the proton in manganite is not covalently bonded to a single oxygen, but lies in the octahedral hole in the center of the tunnel, with 6 O−H interatomic distances of approximately 2 Å.[47] Our NMR results are, however, consistent with a degree of covalent bonding between the deuterons and the oxygen atoms of the tunnel walls, and suggest that the deuteron moves off-center toward one of the oxygen atoms.

At this point, the ambiguity of the proton position in 1 × 2 tunnels of groutite should be mentioned. Hydrogen bonding between O_{sp^3}−H and O_{sp^2} was suggested in many studies based on the short O_{sp^3}−O_{sp^2} bond distance of 2.626 Å, which is appropriate for a hydrogen bond (Figure 1f).[7,19,21] No neutron diffraction data for groutite is, however, available. A neutron diffraction study on diaspore (AlOOH, space group *Pbnm*), which is isostructural with groutite, showed that the proton position did *not* lie midway between the two oxygens.[48] Instead, the O_{sp^3}−H vector makes an angle of 12.1° with the O_{sp^3}−O_{sp^2} tie line, which suggests the absence of strong hydrogen bonding in this compound. The lack of H-bonding is also apparent in the cation(H^+)−anion($O_{sp^2}^{2-}$)−cation(Al^{3+}) bond angle distributions. Angles of 112°, 114°, and 129° are found in the structure of diaspore (AlOOH), while angles of 145°, 100°, and 100° are predicted for hydrogen bonding.[19] The geometry observed for diaspore resembles sp^3-hybridization of the oxygen atoms more closely and is assumed in our discussion below. However, both bonding arrangements result in similar conclusions for the size and direction of the hyperfine shift, within our qualitative discussion of the causes of the shifts.

The ^2H NMR shift of ∼415 ppm of deuterons bonded to the pyramidal oxygens (O_{sp^3}) in the 1 × 2 tunnels of groutite (Figure

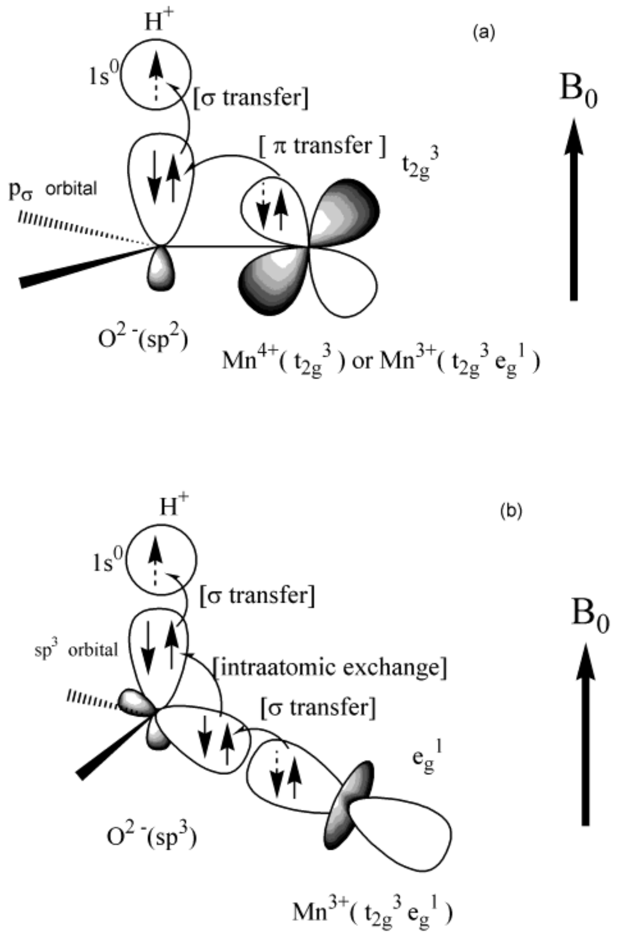

Figure 10. Schematic diagrams showing the transfer of the unpaired electron spin density by two superexchange mechanisms:[41] (a) Unpaired electron spin density is transferred from the half-filled t_{2g}^3-orbitals of the Mn(IV) or Mn(III) ion to the empty 1s-orbital of the proton via pπ−pσ covalent bonds mediated by a fully filled oxygen p-orbital. (b) The unpaired electron spin density is transferred from the half-filled e_g-orbitals of the Mn(III) ion to the empty 1s-orbital of proton via pσ−pσ covalent bonds, mediated and enhanced by the fully filled oxygen sp^3-hybridized orbitals. B_0 represents the external magnetic field, which results in a parallel alignment of the unpaired electrons in the manganese ions.

(43) Nayeem, A.; Yesinowski, J. P. *J. Chem. Phys.* **1988**, *89*, 4600.
(44) Abragam, A.; Bleaney, B. *Electron Paramagnetic Resonance of Transition Ions*; Dover Publication, Inc.: New York, 1986.
(45) Krzystek, J.; Telser, J.; Pardi, L. A.; Goldberg, D. P.; Hoffman, B. M.; Brunel, L.-C. *Inorg. Chem.* **1999**, *38*, 6121.
(46) Lee, Y. J.; Grey, C. P. *Chem. Mater.* **2000**, *12*, 3611.
(47) Fillaux, F.; Cachet, C. H.; Ouboumour, H.; Tomkinson, J.; Levy-Clement, C.; Yu, L. T. *J. Electrochem. Soc.* **1993**, *140*, 585.
(48) Busing, W. R.; Levy, H. A. *Acta Crystallogr.* **1958**, *11*, 798.

4) can be attributed to two different superexchange mechanisms. The superexchange mechanism discussed above involving the t_{2g} orbitals holds in this case, but is expected to be somewhat less efficient, because the cation(H^+)−anion($O_{sp^2}{}^{2-}$)−cation(Mn^{3+}) bond angles deviate significantly from 90° in this sp^3-type atomic arrangement.[41] Another (delocalization) superexchange mechanism is shown in Figure 10b. In this mechanism, p_σ-type covalent bonds form between the fully occupied sp^3-hybridized orbitals of oxygen and half-filled e_g-orbitals of three nearby manganese ions, mediating transfer of electron spin density from the e_g orbitals to oxygen. Spin density is then transferred to the empty 1s-orbital of the deuteron via an intraatomic correlation between the sp^3-hybridized orbitals and the p_σ-type covalent bond between the oxygen and deuterium atoms.[41] A correlation-type superexchange mechanism is also possible, involving a direct interaction of the oxygen p-orbital coordinated to the deuteron, and the e_g orbital; this also results in a positive shift.

It is not easy to quantify, with the data currently available, how much the 90°-cation−anion−cation superexchange mechanism of Figure 10a will decrease as the bond angle deviates to ∼110−120° in the sp^3 configuration, and how much the mechanisms (Figure 10b) involving the e_g orbitals will contribute to the ^2H NMR shift. Nevertheless, it is plausible that the sum of the contribution from the t_{2g} and e_g mechanisms results in a larger ^2H NMR shift of ∼415 ppm for the deuterons bonded to O_{sp^3} in the 1 × 2 tunnels of groutite.

The smaller ^2H NMR shift of 150 ppm from deuterons in vacancy sites of EMD can then be rationalized based on the above discussion. Six oxygens are available for the deuterons (or protons) per (proposed) cation vacancy site: two are axially bonded and four are equatorially bound to the vacant manganese ion. Figure 1b shows the arrangement of two manganese atoms bound to one of these axial oxygens. All of the six oxygens are O_{sp^2}-type when the cation vacancy is located in the pyrolusite domains, while there are three O_{sp^2}- and O_{sp^3}-type oxygens, when the vacancy is located in the ramsdellite domain.[10] Both types of oxygens, regardless of whether the initial configuration was sp^3-type or sp^2-type, are sp^3-hybridized when a deuteron (or proton) replaces the vacant (imaginary) manganese ion. Thus, based on the contribution of each manganese ion to the Fermi-contact shift (100 ppm) calculated above, a ^2H NMR shift of 200 ppm (100 ppm × two Mn^{4+} ions) is estimated, as a first approximation. A decrease in efficiency of the first superexchange mechanism (Figure 10a) is, however, expected since the cation−anion−cation bond angles deviate from ∼90°, and the second superexchange mechanism (Figure 10b) will not occur since the e_g-orbitals are not occupied in the $Mn^{4+}(t_{2g}{}^3e_g{}^0)$ ions, providing an explanation for the smaller observed ^2H NMR shift of 150 ppm for ^2H atoms in the vacancy site.

The ^2H MAS sideband pattern of EMD is quite asymmetric, in contrast to the spectra of groutite and manganite, which show more symmetric sideband patterns. The ^2H NMR line shapes are governed by both the sizes and relative orientations of the tensors that describe the quadrupolar and paramagnetic dipolar interactions.[28,32] Thus, the pronounced asymmetric sideband pattern of EMD can be ascribed to either a quite large dipolar interaction between the ^2H nucleus and unpaired electrons in manganese ions and/or a large deviation in the orientations of the PASs of those two interactions. Our preliminary simulations of these systems, using the approach outlined in the literature,[28,32] suggest that the QCCs in these systems are typical of a rigid deuteron (170−180 kHz), but that dipolar couplings of between 3.5 and 50 kHz are required to simulate the spectra. The larger values are required to simulate the spectra of EMD.

Implications for the Reduction Mechanism. A proton (or electron)-filling mechanism has been suggested for the reduction of manganese ions in the 1 × 2 tunnels in γ-MnO_2.[21] According to this mechanism, the electron inserted along with the proton is delocalized among the e_g orbitals of the nearby manganese ions, at low reduction levels ($MnOOH_x$, $0 < x < 0.5$), but is localized in the d_{z^2}-orbital of one manganese ion (Mn^{3+}) at high reduction levels ($MnOOH_x$, $0.5 < x < 1$). This localization causes (or is due to) the Jahn−Teller distortion of the MnO_6 octahedra, and finally results in the distortion of the 1 × 2 tunnel structures. The electron superexchange mechanisms discussed above are consistent with this electron-filling mechanism, because the e_g-orbital in Figure 10b is not specified, i.e., it could be either the d_{z^2}-orbital of the axially bonded manganese ion (Mn^{3+}) or the $d_{x^2-y^2}$-orbitals of the equatorially bonded manganese ions (Mn^{3+}) at low reduction levels. In other words, similar shifts are predicted for an electron rapidly jumping between the three nearby manganese ions, or for a localized electron in one e_g-orbital at a low reduction level. At a high reduction level, the e_g-orbital in Figure 10b represents the d_{z^2}-orbital of the axially bonded manganese ion (Mn^{3+}). Furthermore, the observation of a discrete resonance (at approximately 415 ppm) at *all* reduction levels in groutite studied provides evidence for the localization of the electron nearby the intercalated proton, rather than delocalization (i.e., hopping) of the electrons over the whole solid.

Deuteron Motion and ^{2}H MAS NMR Line Shapes. Chabre et al. have suggested that the ramsdellite layers or 1 × 2 tunnels in γ-MnO_2 are reduced first in their proton intercalation mechanism. This suggestion was based on a variety of supporting evidence:[7] First, calculations of the electrostatic lattice potentials of manganese and oxygen atoms show that the manganese and oxygen atoms in the ramsdellite domains are more readily reduced and hydroxylated than those in pyrolusite domains. Second, the larger expansion in cell volume required for the rutile-to-manganite transformation ($\Delta V = 5.5$ Å^3/MnO_2) than that for the ramsdellite-to-groutite transformation ($\Delta V = 4.9$ Å^3/MnO_2) suggests that the latter transformation is likely to occur first. This is also consistent with electrochemical studies,[49,50] where the open circuit voltages for the discharge of the β-MnO_2 phase, consisting mainly of 1 × 1 tunnels, have lower potentials of approximately 200 mV than those of the γ-MnO_2 phase, indicating that the 1 × 2 tunnel structures will be reduced at a higher potential, i.e., reduced first. As discussed above, the ^2H NMR spectra of the partially reduced MnO_2 samples, Figure 6a,b, appear to contradict these previous results: the ^2H NMR resonance at 330 ppm, which is assigned to deuterons in the 1 × 1 tunnels, is more intense at low reduction levels than the resonance at 400 ppm, which is assigned to deuterons in 1 × 2 tunnels. Approximate values for the relative intensities of the two resonances of 1:0.5 were measured for the $MnOOD_{0.5}$ sample for the 1 × 1:1 × 2 tunnels, respectively. One possible explanation for this apparent inconsistency is that the different resonances are associated with very different T_2* values. Alternatively, we may be missing some other deuterium spins due to their very short T_2 or T_1 values. These suggestions will now be explored.

It seems unlikely that the "missing" deuterons, whose environments will not differ significantly from the visible deuterons, will have dramatically different T_1 values. Given that

(49) Kozawa, A.; Powers, R. *Electrochem. Technol.* **1967**, *5*, 535.
(50) McBreen, J. *Power Sources* **1975**, *5*, 525.

the T_1 values measured for the visible deuterons in $MnOOD_{0.7}$ (of approximately 10 ms) are quite long, we tentatively conclude that the "missing" deuterons are not a consequence of very short T_1 values. Any differences in the T_2 values of the different resonances due to deuterons in the 1×1 and 1×2 tunnels will alter the apparent relative intensities of the different resonances and thus result in errors in the concentrations of the different environments, as measured by a spin−echo experiment. The measured T_2 values for the two major resonances seen in the spectrum of the $MnOOD_{0.7}$ sample are similar, indicating that the relative intensities of the two resonances reflect the relative concentrations of the two environments. In the case of $MnOOD_{0.5}$, the total signal intensity (i.e., the intensity of the first rotor echo) of $MnOOD_{0.5}$ is only approximately one thirtieth of the intensity of groutite, MnOOD, which cannot be totally explained based on the measured T_2 values of the $MnOOD_{0.7}$, suggesting that we may be missing some deuteron signals due to another phenomenon.

Motion on the appropriate time scale is expected to significantly reduce the ^{2}H signal. For example, the hopping motion of protons throughout the vacancy sites in ice was shown to result in a significant decrease in the signal intensity of a ^{2}H NMR spectrum (acquired with a quadrupolar echo sequence), without affecting the Pake-doublet line shape of the signal, when the correlation time for this motion ranges from $\sim 10^{-4}$ to 10^{-5} s.[24] The diffusion coefficient for mobile protons in slightly reduced γ-MnO_2 has been reported to be 6×10^{-10} cm^2/s,[51] or 6 Å$^2/\mu$s (based on broadline ^{1}H NMR). This proton mobility has been ascribed primarily to the protons attached to pyramidal oxygen (O_{sp^3}), or Coleman protons, in the 1×2 tunnels. Mobility has been reported to decrease as the amount of intercalated protons increases, due to increased repulsion between adjacent protons and the decrease in the available vacant sites for protons.[12] The mobility of these Coleman-type protons in partially reduced γ-MnO_2 samples, and the dependence on the mobility on reduction level, was also suggested by X-ray diffraction experiments:[36] When two partially reduced γ-MnO_2 powder samples, both having different proton intercalation levels, are mixed and firmly packed, the X-ray diffraction lines gradually coalesce. The final X-ray diffraction pattern, collected after about 6 months, shows the same pattern as that of the homogeneous phase having an intermediate proton intercalation level of the two starting samples. The time required for coalescence of the diffraction peaks was observed to be shorter for a mixture of samples with lower intercalation levels, suggesting a higher diffusion rate.

The effect of motion on the signal intensity of spectra acquired by using a rotor synchronized spin−echo sequence may be estimated by using the approach of Maricq and Waugh.[30] Assuming random motions of the deuterons, and using the expression $T_2^* \sim 16(\nu_r/\omega_0\delta)^2\tau_c$, where ν_r is the spinning speed (18 kHz) and $\omega_0\delta$ is the quadrupolar anisotropy ($\sim$170 kHz, derived from simulations of the spectrum), the motion associated with a correlation time (τ_c) of 10^{-3} s results in a T_2^* of approximately 6×10^{-5} s. This will result in noticeable loss of signal intensity (60%) at the first rotor echo (at time $= 5.6 \times 10^{-5}$ s) and considerable loss of intensity at the second rotor period (84%), i.e., at the start of data collection for the spectra shown in Figure 6a. Motion with an even shorter correlation time (τ_c) of 10^{-4} s will result in essentially complete loss of the signal. As the motion increases further, however, the time scale of the motion will enter that of the quadrupole interaction, and averaging of this interaction should now occur, resulting in the reemergence of the signal and a sharp resonance with few or no spinning sidebands. This will occur when $\tau_c \leq 10^{-6}$ s. The D_2O molecules that give rise to the resonance seen in the spectrum of EMD (Figure 3a), prior to dehydration, are clearly undergoing rapid motion in or above this regime (the so-called fast-limit regime).

The loss of intensity in the spectrum of $MnOOD_{0.5}$ in comparison to that of groutite may be due to mobile deuterons that are undergoing motion with $10^{-3} \geq \tau_c \geq 10^{-6}$ s, which are not observable by MAS NMR. A ^{2}H MAS NMR spectrum of $MnOOD_{0.5}$ was acquired at −60 °C to detect any change in deuteron motions at a lower temperature. No significant change in the relative intensity of the isotropic resonance at $\sim$400 ppm and no additional resonances were observed, suggesting that the motion of the "missing" deuterons is still sufficiently fast even at −60 °C. Clearly, spectra need to be collected over a wider temperature range to validate these proposals. Spectra of groutite were, in contrast, acquired over a much wider temperature range (from −120 to 150 °C). Although the overlapping resonances were better resolved at lower temperatures no dramatic disappearances or appearances of new resonances were observed indicating that we are observing all the deuterium spins in this sample. (τ_c for a random motion with an activation energy of $\geq$ 1.5 kJ mol^{-1} will change by more than 3 orders of magnitude over this temperature range and thus any mobile deuterons should be visible at some point in this temperature window; random motions with an even lower activation energy should already be occurring sufficiently fast enough to be in the fast regime of motion, and should therefore be visible by MAS.)

On the basis of the above discussion for groutite, it also appears that we are observing all the deuterons in EMD (at least below 100 °C). No evidence for Coleman-type (mobile) protons, other than those in the form of adsorbed molecular water, is observed in the ^{2}H MAS NMR spectra of our deuterated EMD sample (Figure 3). Given a typical manganese-to-oxygen ratio in EMD of 1:1.95−1.97, the MnO_2/MnOOH ratio lies somewhere between $19MnO_2 \cdot MnOOH$ and $8MnO_2 \cdot MnOOH$. In contrast the Mn:vacancy ratio is approximately 1:0.05. Thus, assuming that there are four deuterons per Mn^{4+} vacancy, there are approximately 0.20 deuterons associated with the vacancies, and 0.05 to 0.12 deuterons associated with the Mn(III), per MnO_x formula unit.[9] Thus, it may be that we do not have the sensitivity to detect these protons. Alternatively, it may be that these protons are present in much lower concentrations in our preparation of EMD.

The disappearance of the signal assigned to the Ruetschi deuterons above 150 °C is ascribed to deuterium motion. The motion of the deuterons clearly enters the time scale of the magic angle spinning (i.e., $\tau_c < 10^{-3}$ s) above 150 °C. The occurrence of motion in this system is consistent with the change in the T_2^* values with temperature for the Ruetschi deuterons: From −100 to 30 °C, the T_2^* values increase (i.e., the line widths decrease), consistent with the decrease in the magnetic moments of the manganese ions as the temperature is raised. This behavior was seen for all the samples studied. Unlike the T_2^* values for groutite and manganite, a reversal in this trend is seen above room temperature. This is ascribed to a contribution to the T_2^* due to motion. Assuming that motion dominates the T_2^* at 150 °C, a correlation time of 1.3 ms may be estimated (again assuming a random motion, and using $\nu_r \sim$10 kHz and $\omega_0\delta$ $\sim$170 kHz). This estimate represents a lower limit for the correlation time at this temperature. The observation of a signal

(51) Kahil, H.; Dalard, F.; Guitton, J.; Cohen-Addad, J. P. *Surf. Technol.* **1982**, *16*, 331.

with a T_2* of 0.25 ms at room temperature means that the deuterons cannot be associated with a correlation time (τ_c) of less than 4.5 ms. Our results do not agree with the previous INS studies:[47,52,53,54] Here, Fillaux et al. observed Ruetschi protons in crystal defects of EMDs. These protons were suggested to be mobile at room temperature in the INS time scale (10^{-12} s).[53] This dramatic difference between the INS and NMR studies cannot solely be ascribed to a kinetic isotope effect.

Conclusions

This work has demonstrated that high-resolution deuterium NMR may be used to probe the local environment of deuterons in highly defective paramagnetic materials. These systems represent materials where diffraction techniques are of limited value for determining the locations of these protons, but where the concentration, nature, and locations of the protons dramatically alter the effectiveness of the material as a cathode in a primary battery.

The so-called Ruetschi deuterons have been detected by NMR, for the first time, in deuterated EMD; these deuterons give rise to a ^{2}H NMR resonance at 150 ppm at room temperature, with a large spinning sideband manifold due to a rigid O−D group. These deuterons are also rigid on the ^{2}H MAS NMR time scale (i.e., $\tau_c > 10^{-3}$ s), in contrast to earlier (INS) studies of the protonated systems that indicated that the protons were extremely mobile. The temperature dependence of the shift and the MAS NMR line shape of this resonance indicate that both the structural and electronic environments of these deuterons are very different from those associated with Mn^{3+} ions in the 1 × 1 channels of manganite or the 1 × 2 channels of groutite (the Coleman deuterons). Above 150 °C, the signal from these deuterons disappears indicating that the deuterons are no longer rigid in the MAS time scale but are associated with a correlation time for motion of $\leq 10^{-3}$ s. No Coleman protons were observed in EMD, presumably due to their low concentration, and possibly because of their proposed mobility.

Much larger ^{2}H NMR shifts of ∼300 and ∼415 ppm were observed for the deuterons in the tunnel structures of manganite and groutite, which were ascribed to a Fermi contact interaction caused by an electron spin delocalization superexchange mechanism. The different shifts were rationalized by considering the different bonding arrangements for deuterium in the 1 × 1 and 1 × 2 tunnels. The smaller shift seen for the EMD deuterons was ascribed to the smaller number of manganese ions in the local coordination sphere. Almost identical shifts were seen at different intercalation levels, consistent with the localization of the electron associated with the deuteron in the e_g-orbitals of the adjacent manganese ions, rather than delocalization throughout the solid.

The spectra of groutite synthesized from both an artificial ramsdellite or EMD showed deuterons in both the 1 × 1 and 1 × 2 tunnels. Interestingly, even at a 50% intercalation level, deuterons were still observed in the 1 × 1 tunnels, when using the reduction agent cinnamyl alcohol. These results should be compared to previous work, which suggested that the 1 × 1 tunnels should be much more difficult to intercalate, and thus might only be intercalated at higher reduction levels. Our work suggests that intercalation of the 1 × 1 tunnels of these highly defective structures may be much easier than intercalation of the 1 × 1 tunnels of highly crystalline structures, presumably the defects providing both easy intercalation pathways and greater flexibility of the structure toward deuterium incorporation. In agreement with this suggestion, deuterium intercalation of pyrolusite, using the same procedure used to intercalate ramsdellite, yielded no detectable ^{2}H signal.

Variable-temperature NMR of these systems showed a Curie−Weiss-like dependence on temperature for the hyperfine shifts of EMD and groutite, but very little dependence on temperature for the shift of the manganite deuterons, consistent with the strong antiferromagnetic correlations that exist for this latter compound above the Néel temperature. The different temperature dependences of the shift could be used to identify the presence of larger manganite-like domains within the sample of ramsdellite, which were either too small or present in too low concentrations to be detected by X-ray diffraction.

Work is now in progress to examine in more detail the concentrations, nature, and mobility of the different deuteron sites in a range of EMD samples and the role that these sites play in controlling the subsequent reduction process. Extensions of this approach to the study of a wide range of cathode (e.g., nickel hydroxide) or intercalated materials may be readily envisaged. Furthermore, the use of deuterium NMR to test, for example, possible failure mechanisms in cathode materials that involve proton intercalation into the host materials appears to be a feasible method.

Acknowledgment. This work was performed with support from Duracell, Inc. and the National Science Foundation (DMR 9901308). C.P.G. is an Arthur P. Sloan Research Fellow.

JA015999K

(52) Fillaux, F.; Ouboumour, H.; Tomkinson, J.; Yu, L. T. *Chem. Phys.* **1991**, *149*, 459.
(53) Fillaux, F.; Ouboumour, H.; Cachet, C.; Kearley, G. J.; Tomkinson, J.; Yu, L. T. *Chem. Phys.* **1992**, *164*, 311.
(54) Fillaux, F.; Cachet, C. H.; Ouboumour, H.; Tomkinson, J.; Levy-Clement, C.; Yu, L. T. *J. Electrochem. Soc.* **1993**, *140*, 592.